Journal of Maps

ISSN: (Print) 1744-5647 (Online) Journal homepage: https://www.tandfonline.com/loi/tjom20

New bathymetry of the Linosa volcanic complex from multibeam systems (Sicily Channel, Mediterranean Sea)

Renato Tonielli, Sara Innangi, Gabriella Di Martino & Claudia Romagnoli

To cite this article: Renato Tonielli, Sara Innangi, Gabriella Di Martino & Claudia Romagnoli (2019) New bathymetry of the Linosa volcanic complex from multibeam systems (Sicily Channel, Mediterranean Sea), Journal of Maps, 15:2, 611-618, DOI: 10.1080/17445647.2019.1642807

To link to this article: https://doi.org/10.1080/17445647.2019.1642807

JOURNAL OF MAPS
2019, VOL. 15, NO. 2, 611–618
https://doi.org/10.1080/17445647.2019.1642807

Science

OPEN ACCESS Check for updates

New bathymetry of the Linosa volcanic complex from multibeam systems (Sicily Channel, Mediterranean Sea)

Renato Tonielli [a], Sara Innangi [a], Gabriella Di Martino [a] and Claudia Romagnoli [b]

[a]Istituto di Scienze Marine del CNR, Napoli, Italy; [b]Dipartimento di Scienze Biologiche, Geologiche ed Ambientali, Università di Bologna, Bologna, Italy

ABSTRACT

This paper presents new bathymetric data acquired around Linosa Island, in the Pelagie Archipelago, revealing the submarine extension of the volcanic edifice, more wide and complex than previously known. The seafloor of Linosa, from the coastal area to about 1000 m depth, was mapped with multibeam systems during the 'Linosa 2016' and 'BioGeoLin 2017' surveys. A bathymetric map of the surveyed area (about 298 km^2) was drawn at the original 1:30,000 scale. Overall, the submarine portions of Linosa extend on a total area of about 159 km^2 and are preferentially developed in a NW-SE direction, in agreement with the regional main tectonic trend in the area. The new bathymetric data allow to recognize different sectors in the submarine extension of the volcanic edifice where constructional (volcanic) activity alternates with erosive-depositional processes affecting the submarine flanks of the island.

ARTICLE HISTORY
Received 23 November 2018
Revised 9 July 2019
Accepted 9 July 2019

KEYWORDS
Multibeam bathymetry; volcanic island; Pelagie islands

1. Introduction

While recent advances in seafloor imagery systems enabled the extensive mapping of the seafloor, enlarging the knowledge of submarine volcanic areas (Casalbore, 2018) we are still far from having a complete coverage of the submarine portions of many volcanic islands, which commonly represent the limited emerged tips of much larger volcanic edifices. The submarine portions of Linosa Island, in the Pelagie Archipelago, were scarcely known up to now, apart from early studies carried out in the 1988–1992 by the University of Bologna with conventional, single-channel echosounder (Romagnoli, 2004; Rossi, Gabbianelli, Romagnoli, & Serri, 1990). These early data showed the uneven extension of the volcanic structure, aligned in NW-SE direction and surrounded by minor submarine eruptive centers, but they only extended to about 500 m of depth, leaving unknown great part of the volcanic edifice. The Pelagie Archipelago, composed by Lampedusa and Linosa Islands and Lampione Islet, is located in the Sicily Channel (central Mediterranean Sea, Italy) at halfway between Sicily and Lybia (35°30′13″N–12°36′25″E; Figure 1; Innangi, Di Martino, Romagnoli, & Tonielli, 2019; Innangi et al., 2018). Water depths of the Sicily Channel are general less than 400 m, except in the three NW-SE trending grabens of Pantelleria (PG), Linosa (LG) and Malta (MG) formed in the Neogene-Quaternary in a context of continental rifting (Civile et al., 2010; Dart, Bosence, & McClay, 1993; Finetti, 1984; Maldonado & Stanley, 1977). The aim of this work is to present the new bathymetric data acquired around Linosa island, which represents the emerging summit of a larger volcanic complex lying on the western shoulder of the Linosa graben (Grasso et al., 1991; Figure 1). The island has a surface area of about 5.4 km^2 and a maximum elevation of about 195 m above sea level (Innangi et al., 2018). The subaerial volcanic activity of Linosa ages back to 1.06–0.53 Ma and has been divided into three main eruptive stages, during which hydromagmatic and magmatic eruptions produce tuff rings, tuff cones, scoria and spatter cones and extended lava flows (Grasso & Pedley, 1985, 1988; Lanzafame, Rossi, Tranne, & Lanti, 1994; Rossi, Tranne, Calanchi, & Lanti, 1996). No data are available, instead, for the age of its wide submarine portions. The distribution of the meso-structures and of the eruptive centers on the island suggests that the NNW–SSE and the WNW–ESE are the main and secondary trends, respectively, along which a significant tectonic control occurred on the development of volcanic activity (Grasso et al., 1991; Lanti, Lanzafame, Rossi, Tranne, & Calanchi, 1988; Lanzafame et al., 1994). According to the paleo-morphological reconstruction and volcano stratigraphy (pyroclastic deposits distribution and provenance) on Linosa, some of its eruptive centers were located at sea, on the shallower SE and NW flanks of the island (Lanti et al., 1988; Lanzafame et al., 1994). This is in agreement with the location of wide insular shelves were observed at depth less than −120 m, giving indications on the original extension of

CONTACT Sara Innangi sara.innangi@cnr.it Istituto di Scienze Marine del CNR, Calata Porta di Massa, 80, 80133 Napoli, Italy

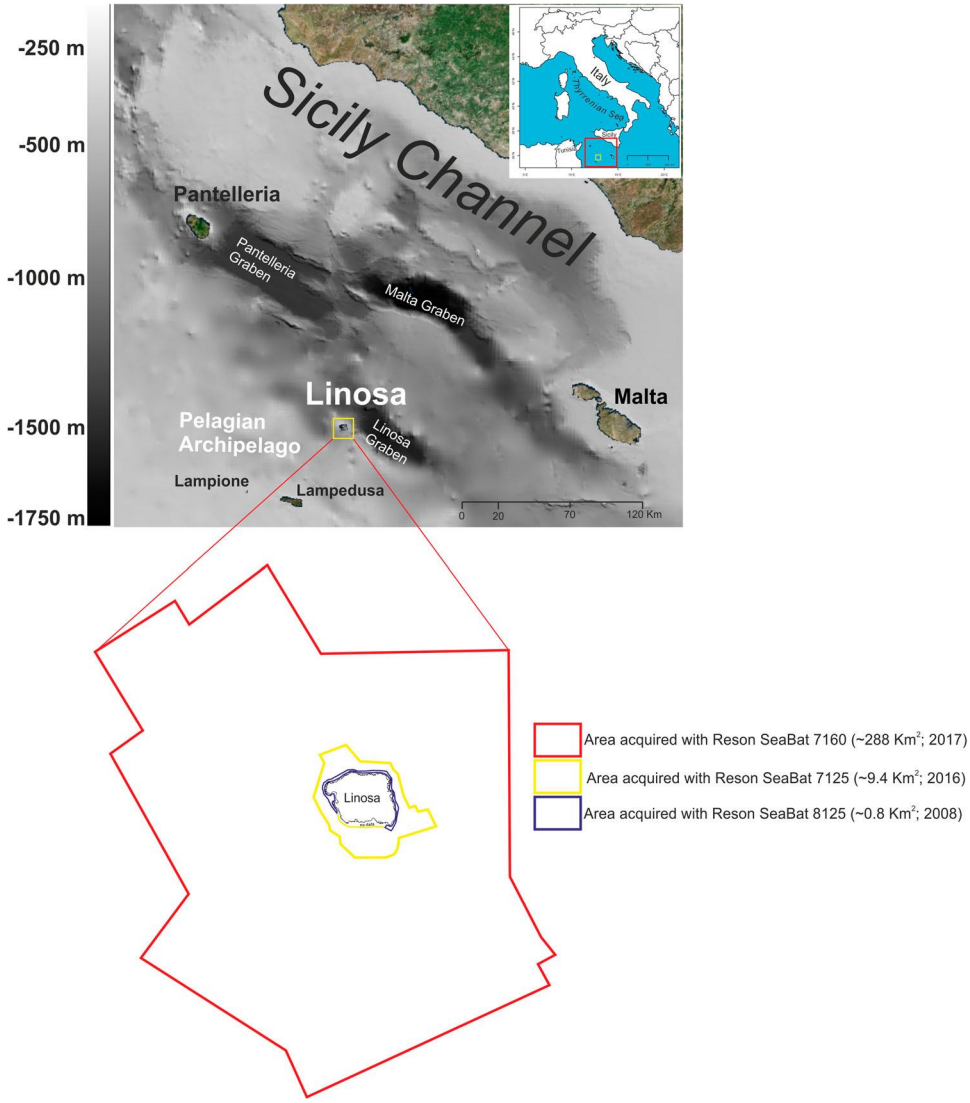

Figure 1. Location Map of Linosa Island in the Sicily Channel (above) and indication of surveyed areas (below) during the 'Linosa 2016' survey (in yellow) and the 'BioGeoLin 2017' survey (in red). The extension of previously acquired bathymetric shallow-water data is also indicated (in blue).

the early volcanic edifice, largely dismantled by marine erosion during Late-Quaternary sea-level fluctuations (Romagnoli, 2004). The new, high-resolution bathymetric map presented here, at 1:30,000 scale (see Main Map), allows to enlarge and better define the submarine structure of the Linosa volcanic edifice, showing a wider and more articulated extension with respect to what previously known.

2. Methods

2.1. Acoustic data acquisition and processing

Geophysical data were collected by the Institute for Coastal Marine Environment (IAMC, now ISMAR, Institute of Marine Sciences) of the National Research Council (CNR) of Naples (Italy) during two oceanographic surveys, 'Linosa 2016' (17–29 August 2016) and 'BioGeoLin 2017' (8–20 September 2017), onboard the R/V *Minerva UNO* (Di Martino et al., 2017; Innangi & Tonielli, 2017). Multibeam bathymetric surveys were carried out around Linosa Island from about 15 to 1000 m of depth, obtaining the almost whole coverage of its submarine flanks down to the base of the volcanic edifice and in surrounding areas (Figure 1). The shallow-water survey was performed from 15 to about 180 m of depth using a Teledyne Reson SeaBat 7125 (Figure 1, area in yellow) while the seabed down to 1000 m of depth was investigated using a Teledyne Reson SeaBat 7160 (Figure 1, area in red). The technical specifications of the two adopted multibeam systems are summarized in Table 1.

Bathymetric data were collected and processed using Teledyne PDS 4.1; the software received positioning information from an Ominstar Differential Global Positioning System (DGPS) and attitude data from an Ixea Octans 3000 motion sensor. Sound velocity values at multibeam transducers were provided by a Valeport mini-SVS probe, while a sound velocity profiler was systematically used to get the velocity profile in the

Table 1. Technical specifications for the multibeam systems adopted in the surveys.

Teledyne Reson SeaBat 7125	
Frequency	400 kHz
Max ping rate	50 Hz
Along-track transmit beamwith	1°
Across-track receive beamwith	0.5°
Pulse length	30–300 μs Continous Wave 300 μs–20 ms Frequency Modulated (X-Range)
Number of beams	512 EA/ED at 400 kHz
Max swath angle	140° in Equi-Distant Mode 165° in Equi-Angle Mode
Typical depth	0.5–150 m at 400 kHz
Max depth	>175 m at 400 kHz
Depth resolution	6 mm
Teledyne Reson SeaBat 7160	
Frequency	44 kHz
Max ping rate	50 Hz
Along-track transmit beamwith	1.5°
Across-track receive beamwith	2° at nadir
Pulse length	30–300 μs Continous Wave 300 μs–20 ms Frequency Modulated (X-Range)
Number of beams	512 ED/150 EA
Max swath angle	Greater than 4x water depth
Typical depth	3–3000 m
Max depth	3000 m
Depth resolution	12 cm

water column. Both measurements are required for a proper depth computation. During the surveys various filter settings were applied to the multibeam data and quality control displays were used to check the data quality; data logging progress was shown in real-time using a color-coded Digital Terrain Model (DTM). The PDS Editing combines in a single module 3D swath editing, multibeam calibration, DTM editing and SVP editor and it allows to clean swath data and to update DTM model in real-time. Data de-spiking was carried out manually without the application of automatic filters in order to preserve data accuracy and resolution. Bathymetric data, previously collected in very shallow-water in the framework of a mapping project, were also available (Coastal Consulting Exploration s.r.l., 2008; Figure 1, blue area). This latter dataset was acquired in 2008 using Reson SeaBat 8125 and was integrated with the new data in order to expand the bathymetric map towards the coast (less than 15 m of the depth). These data were acquired only within the Pelagie Marine Protected Area (Innangi et al., 2018; Tonielli, Di Martino, & Innangi, 2017). Therefore, in the southern sector, which is not included in the MPA, the bathymetric data are missing in the range from 20 m to the coast (Figure 1).

3. Results and discussion

All available data were merged to create a bathymetric map of Linosa, drawn at the original scale of 1:30.000 (see Main Map). The final DTM (10 × 10 m cell grid size) shows that the volcanic edifice is mostly extended below sea level and much larger than the small area of the island (Figure 2). The depth of the base of the volcanic complex extends, in fact, down to at least −1000 m to the north and north-east, −750 m to the west and east, and about −400/−450 m to the south. This is due to the different setting of the submarine flanks of the volcanic edifice, hereafter described according to an informal division in four main sectors (Figure 3). The overall extension of the submarine portions of Linosa is the widest along the NW–SE direction, reaching about 20 km. Sector NW (Figure 3) is characterized by a number of minor, submarine eruptive centers, mostly aligned along a volcanic belt, and it is composed by more than 20 individual eruptive centers lying at different depth (Belvisi, 2018; 3D view in Figure 4(a)). Two of these have the summit in relatively shallow-water, i.e. 'Secca Maestra' and 'Secca di Tramontana', the two main shoals in Figure 4(a). The former is a conical eruptive center with the summit at −38 m, while the second is a sub-circular morphological volcanic structure strongly eroded, lying between 40 and 20 m of depth on the insular shelf surface (Figure 4(a)). On the opposite side of the island (Sector S in Figure 3), the southern submarine flank of Linosa has a sub-rounded shape and is less deep than the northern one (see 3D view in Figure 4(b)). A number of eruptive centers are present on the southern submarine flank of the island, rising from depth between −250 and −570 m (Figure 4(b)) and damming small intra-slope basins (Belvisi, 2018; Romagnoli, 2004). They are roughly arranged in a semi-circular pattern around the island, although local NNW–SSE to WNW–ESE alignments are recognizable in their distribution. The former alignment can be observed, for instance, in the flattened and strongly eroded remnants of minor eruptive centers (with top at −33 and −30 m, respectively, in Figure 4(b) and Innangi et al., 2018) observed in shallow-water, on the insular shelf to the SE of the island, having here an outer edge at about −100 m. Previous works (Innangi et al., 2018; Romagnoli, 2004) described the shelf in the southern submarine sector as being covered by volcaniclastic deposits arranged in terraced, prograding depositional bodies. The smoothness of the shelf surface reflects, in fact, the sedimentary coverage, likely fed by reworked volcaniclastic material due to the erosion of pyroclastic and lava units on the island, a process commonly observed in the post-eruptive, degradational stage of insular volcanoes (Romagnoli & Jakobsson, 2015). Finally, on the southeastern flank of the island, between about −300 and −450 m, a lava field is present, giving place to an irregular seabed with relatively fresh morphology (Figure 4(b)). A peculiar feature to the south-west of Linosa island is a main scarp in the seabed, about 9 km long, developed between −500 and −700 m in an NW–SE direction (Figure 4(b)). It delimits the volcanic edifice westwards, being likely tectonically controlled (see also Figure 2). The north-eastern and

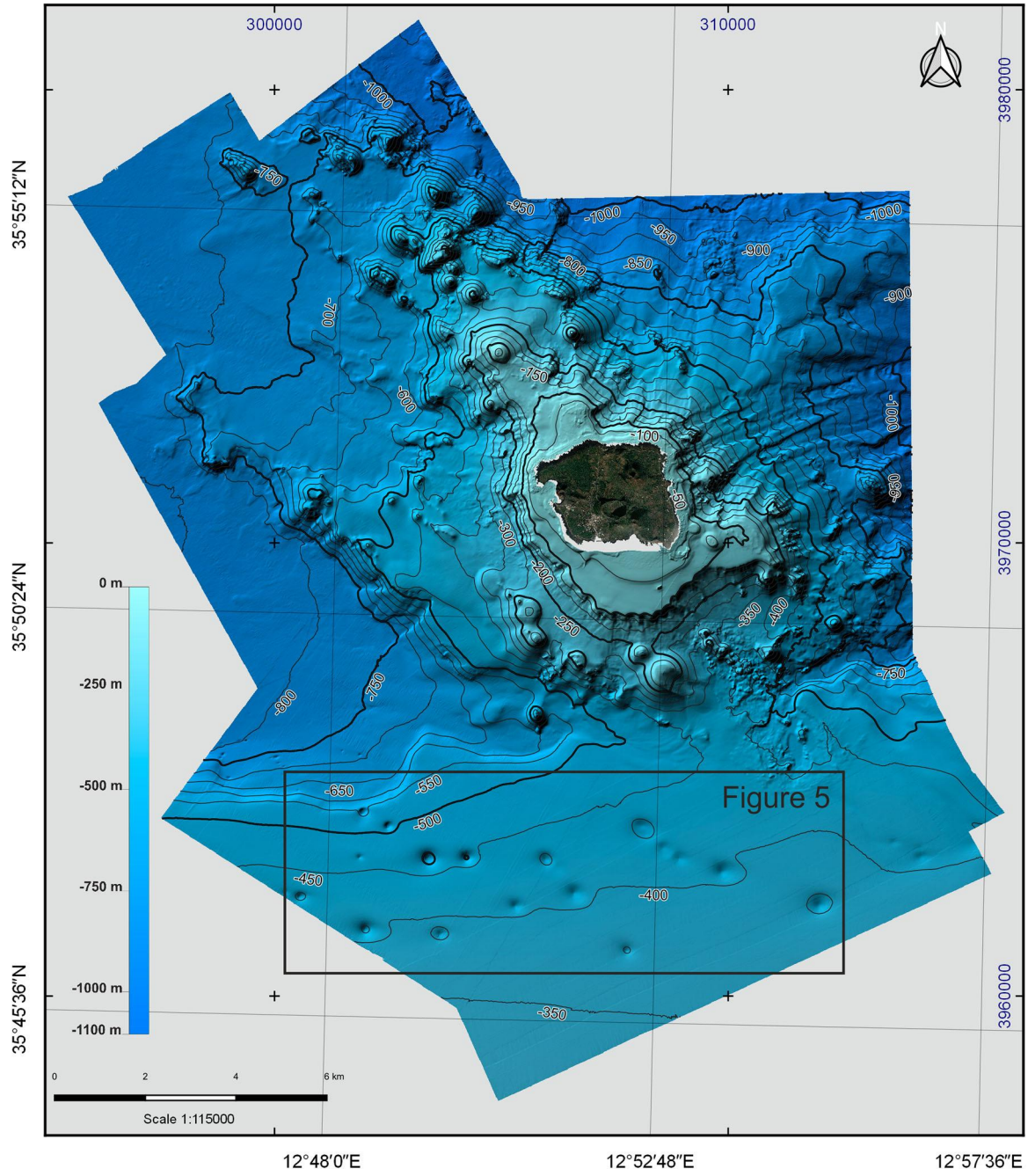

Figure 2. Shaded relief image of the bathymetric data of Linosa Island (10 × 10 m cell grid size).

western submarine flanks of Linosa Island (sectors NE and W in Figure 3) are, instead, characterized by erosive processes, as witnessed by the presence of active canyons with their heads in shallow-water (where insular shelves are lacking, see the 3D views in Figure 4(c,d)), alternating with sub-radial volcanic structures and outcrops, representing the eroded remnants of constructional volcanic features (Chadwick et al., 2005; 3D view in Figure 4(c)). An irregular, small lava field with irregular morphology is observed to the north-east of the island, at depth varying between −856 and −988 m, covering a total area of 2.27 km^2 (Belvisi, 2018; Figure 4(c)). For what regards the canyons, the occurrence in their bottom of crescent-shaped bedforms with crest-lines trending roughly perpendicular to the slope direction (Figure 4(c)) suggests that they are seat of active reworking processes, as also observed in other submarine volcanic context such as in the Aeolian Islands (Casalbore, Bosman, Romagnoli, & Chiocci, 2017). Finally, in the southern area of Linosa from the base of the volcanic edifice towards the south, the seafloor decreases in a flat, gradually sloping area (at 500–400 m depth) showing the presence of several circular depressions, about 130–600 m wide and over 50 m deep (Figure 5), partly aligned along the NW–SE direction. This can be identified as a pockmark field, similarly to what observed in other areas of the Mediterranean Sea (e.g. Spatola, Micallef, Sulli, Basilone, & Basilone, 2018), probably due to rising fluids (Ingrassia et al., 2015; Misuraca et al., 2018; Nardelli et al., 2017).

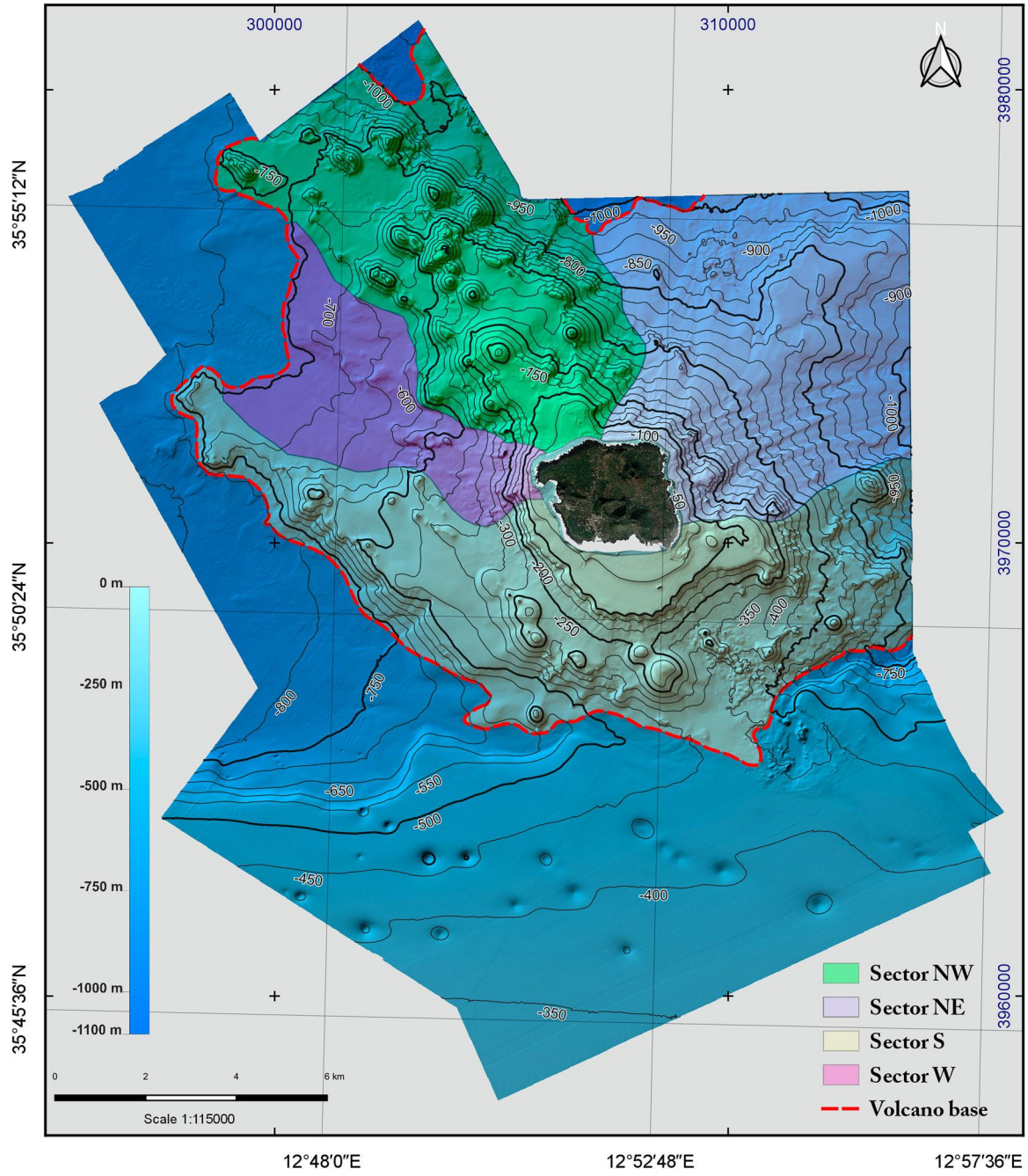

Figure 3. Shaded relief image of the bathymetric data of Linosa Island with indication of the four main sectors described in the text. The morphological base of the volcanic edifice is also indicated.

Further investigations are necessary to better understand the nature of these features.

4. Conclusions

The volcanic island of Linosa has an area of 6 km^2 and represents only a small percentage (about 3.6%) of the entire volcanic complex (about 165 km^2). This first bathy-morphological analysis of the multibeam data recently acquired around the island allows to improve the knowledge of the submarine extension of the Linosa volcanic complex and of its submarine development. In particular, the new data enhance the fundamental role, in the growth of the submarine portions of the volcanic edifice, played by the NW–SE oriented regional tectonic trend in controlling the subaerial and submarine volcanic activity (Lanti et al., 1988; Rossi et al., 1990). Overall, it is possible to define different sectors in the submarine extension of the volcanic edifice, having distinctive characteristics:

- The north-western and southern submarine flanks are characterized by the widespread occurrence of secondary eruptive centers: these in the NW of the island are distributed along a volcanic belt that extends for over 8 km in an NW–SE direction, while to the south they are distributed in a semi-circular arrangement with respect to the island, being partly aligned along the same trend.

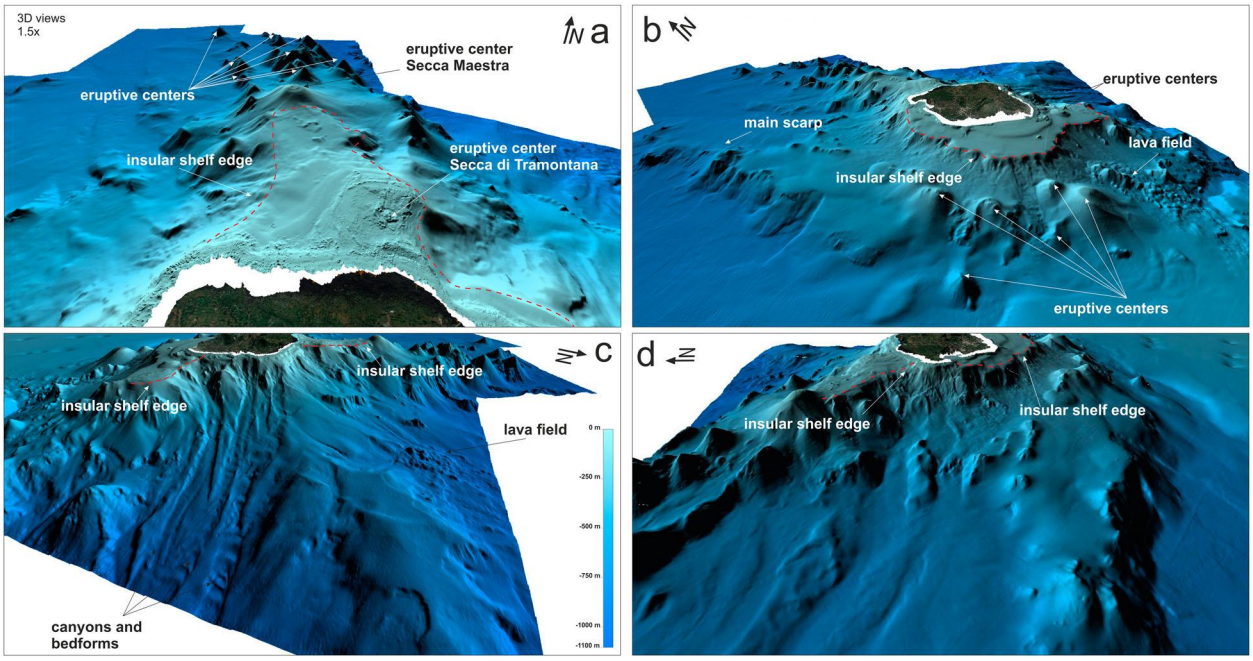

Figure 4. 3D views (vertical exaggeration 1.5x) of the four submarine sectors individuated in the Linosa volcanic complex: north-western sector (a), southern sector (b), north-eastern sector (c), western sector (d). See text for details.

- In the eastern/north-eastern and western submarine flank, on the other hand, erosive and depositional processes prevail, as witnessed by the presence of a network of active canyons from shallow-water to the submarine base of the volcanic edifice. This is partly due to the absence of a well-developed insular shelf in this sector disconnecting the subaerial and the submarine portions, while reworking processes are promoted on these steep submarine flanks.

An important lineament of likely tectonic origin delimits the south-western submarine flank at depth of 500–700 m; its NW–SE orientation is in agreement with the main regional structural systems in the Sicily Channel and in the nearby Linosa graben (Grasso et al., 1991). Similar preferential alignment is shown by several fluid-escape features (pockmarks) observed in the area to the south of the island base, suggesting a structural control on these processes. These features

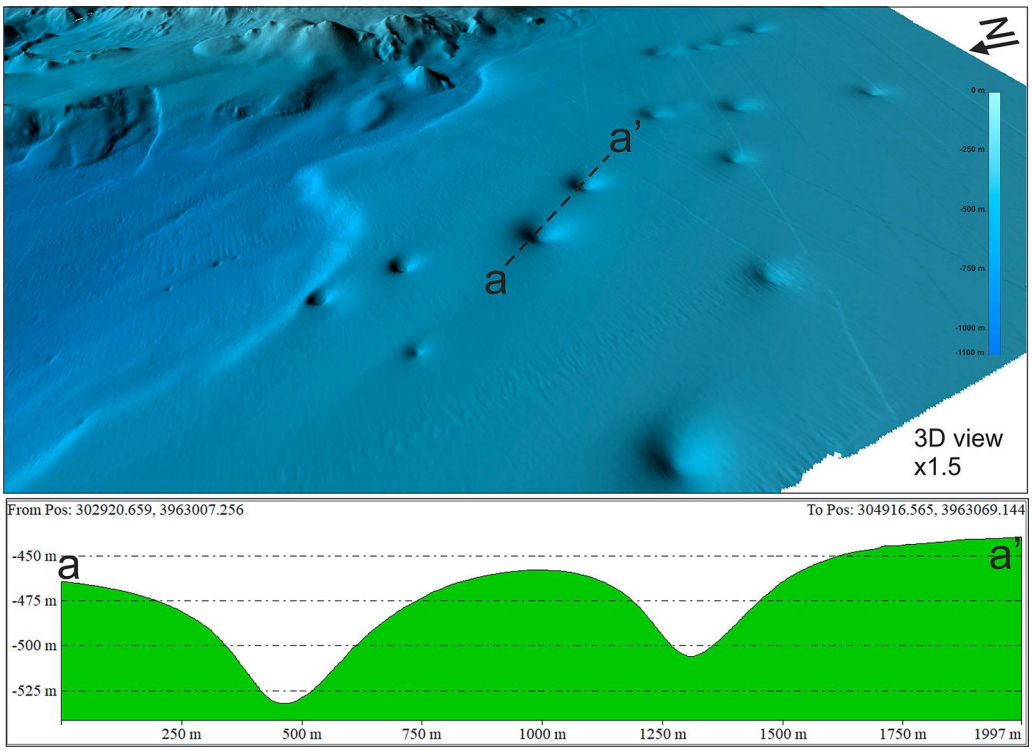

Figure 5. 3D view (from the W) of the pockmark field identified to the south of Linosa (location in Figure 2). Below, the bathymetric section a–a′ crosses two pockmarks (about 40–50 m deep, and width between 250 and 500 m).

will thus require further investigation in order to better characterize the interaction with active tectonics.

To conclude, the new bathymetric map of Linosa presented here represents a first base for future investigation on the growth and evolution of this volcanic island, whose wide submarine portions are still largely unknown.

Software

Bathymetric data were acquired and processed with Teledyne PDS 4.1, as well as the final DTM. The 3D views were produced with Global Mapper cartographic software. The Main Map was produced using QGIS NOOSA 3.6.2.

Acknowledgements

Thanks to the crew of the R/V 'Minerva Uno', for all the support during board and research operations.

Disclosure statement

No potential conflict of interest was reported by the authors.

Funding

This study benefited from contribution of the project 'Implementation of research activity and monitoring around Pelagie Islands Marine Protected Area', within the project 'CAmBiA – Contabilità Ambientale e Bilancio Ambientale' funded by the Ministry of the Environment and Protection of Land and Sea (also known as MATTM – Ministero dell'Ambiente e della Tutela del Territorio e del Mare), Directive n° 5135 of March 2015. This study also benefited from the contribution of the RITMARE (La Ricerca ITaliana per il MARE – http://www.ritmare.it/) Flagship Project, funded by Ministry of Education, University and Research (also known as MIUR – Ministero dell'Istruzione dell'Università e della Ricerca) [NRP 2011–2013].

ORCID

Renato Tonielli http://orcid.org/0000-0002-8792-9511
Sara Innangi http://orcid.org/0000-0002-7692-9356
Gabriella Di Martino http://orcid.org/0000-0001-6630-3432
Claudia Romagnoli http://orcid.org/0000-0002-1585-5525

References

Belvisi, V. (2018). *Studio morfologico e morfometrico delle strutture vulcaniche sottomarine di Linosa* (Master's degree thesis). Alma Mater Studiorum A.D. 1088 Università di Bologna.

Casalbore, D. (2018). Volcanic islands and seamounts. In A. Micallef, S. Krastel, & A. Savini (Eds.), *Submarine geomorphology* (Submarine). Cham: Springer. doi:10.1007/978-3-319-57852-1_17

Casalbore, D., Bosman, A., Romagnoli, C., & Chiocci, F. L. (2017). Small-scale bedforms generated by gravity flows in the Aeolian Islands. In J. Guillén, J. Acosta, F. L. Chiocci, & A. Palanques (Eds.), *Atlas of bedforms in the western Mediterranean* (pp. 287–292). Cham: Springer. doi:10.1007/978-3-319-33940-5_44

Chadwick, W. W., Embley, R. W., Johnson, P. D., Merle, S. G., Ristau, S., & Bobbitt, A. (2005). The submarine flanks of Anatahan Volcano, commonwealth of the northern Mariana Islands. *Journal of Volcanology and Geothermal Research*, *146*(1–3), 8–25. doi:10.1016/j.jvolgeores.2004.11.032

Civile, D., Lodolo, E., Accettella, D., Geletti, R., Ben-Avraham, Z., Deponte, M., … Romeo, R. (2010). The Pantelleria graben (Sicily Channel, central Mediterranean): An example of intraplate 'passive' rift. *Tectonophysics*, *490*(3–4), 173–183. doi:10.1016/j.tecto.2010.05.008

Coastal Consulting Exploration s.r.l. (2008). *Relazione su rilievi marini finalizzati allo studio della morfologia e batimetria dei fondali dell'Isola di Linosa*. Internal Technical Report of Marine Protected Area, Lampedusa, Italy.

Dart, C. J., Bosence, D. W. J., & McClay, K. R. (1993). Stratigraphy and structure of the Maltese graben system. *Journal of the Geological Society*, *150*(6), 1153–1166.

Di Martino, G., Tonielli, R., Innangi, S., Romagnoli, C., Di Stefano, M., Grasselli, F., … Scarpati, V. (2017). *Rapporto di fine Campagna 'BioGeoLin'*. CNR-SOLAR, 20 pp. Retrieved from http://eprints.bice.rm.cnr.it/identificationcode8824TR2018, http://eprints.bice.rm.cnr.it/17164/

Finetti, I. (1984). Geophysical study of the Sicily Channel rift zone. *Bollettino Di Geofisica Teorica e Applicata*, *26*, 3–28.

Grasso, M., Lanzafame, G., Rossi, P. L., Schmincke, H.-U., Tranne, C. A., Lajoie, J., & Lanti, E. (1991). Volcanic evolution of the Island of Linosa, Strait of Sicily. *Geological Society of Italy, Memoir*, *47*, 509–525.

Grasso, M., & Pedley, H. M. (1985). The Pelagian Islands: A new geological interpretation from sedimentological and tectonic studies and its bearing on the evolution of the central Mediterranean Sea (Pelagian Block). *Geologica Romana*, *24*(11), 13–34.

Grasso, M., & Pedley, H. M. (1988). *Carta geologica dell'isola di Lampedusa (Isole Pelagie, Mediterraneo Centrale) 1/10,000*. Cartographie: SELCA, Florence.

Ingrassia, M., Martorelli, E., Bosman, A., Macelloni, L., Sposato, A., & Chiocci, F. L. (2015). The Zannone Giant Pockmark: First evidence of a giant complex seeping structure in shallow-water, central Mediterranean Sea, Italy. *Marine Geology*, *363*, 38–51. doi:10.1016/j.margeo.2015.02.005

Innangi, S., Di Martino, G., Romagnoli, C., & Tonielli, R. (2019). Seabed classification around Lampione islet, Pelagie Islands marine protected area, Sicily Channel, Mediterranean Sea. *Journal of Maps*, 1–12. doi:10.1080/17445647.2019.1567401

Innangi, S., & Tonielli, R. (2017). *Relazione finale della Campagna Oceanografica 'Linosa'*. CNR-SOLAR, 20 pp. Retrieved from http://eprints.bice.rm.cnr.it/identificationcode8361TR2017, http://eprints.bice.rm.cnr.it/

Innangi, S., Tonielli, R., Romagnoli, C., Budillon, F., Di Martino, G., Innangi, M., … Lo Iacono, C. (2018). Seabed mapping in the Pelagie Islands marine protected area (Sicily Channel, southern Mediterranean) using remote sensing object based image analysis (RSOBIA). *Marine Geophysical Research*. doi:10.1007/s11001-018-9371-6

Lanti, E., Lanzafame, G., Rossi, P. L., Tranne, C. A., & Calanchi, N. (1988). Vulcanesimo e tettonica nel Canale di Sicilia: L'isola di Linosa. *Mineralogica et Petrographica Acta*, *31*, 69–93.

Lanzafame, G., Rossi, P. L., Tranne, C. A., & Lanti, E. (1994). *Carta geologica dell'isola di Linosa 1: 5000*. SELCA.

Maldonado, A., & Stanley, D. J. (1977). Lithofacies as a function of depth in the Strait of Sicily. *Geology*, *5*(2), 111–117. doi:10.1130/0091-7613(1977)

Misuraca, M., Budillon, F., Tonielli, R., Di Martino, G., Innangi, S., & Ferraro, L. (2018). Coastal evolution, hydrothermal migration pathways and soft deformation along the Campania continental shelf (southern Tyrrhenian Sea): Insights from. *Geosciences Journal*, *8*(121), 1–22. doi:10.3390/geosciences8040121

Nardelli, B. B., Budillon, F., Watteaux, R., Ciccone, F., Conforti, A., De Falco, G., … Iudicone, D. (2017). Pockmark morphology and turbulent buoyant plumes at a submarine spring. *Continental Shelf Research*, *148* (September), 19–36. doi:10.1016/j.csr.2017.09.008

Romagnoli, C. (2004). Submerged depositional terraces around Linosa Island (Sicily Channel). In *APAT – Memorie descrittive della Carta Geologica D'Italia* (pp. 71–74).

Romagnoli, C., & Jakobsson, S. P. (2015). Post-eruptive morphological evolution of island volcanoes: Surtsey as a modern case study. *Geomorphology*, *250*, 384–396. doi:10.1016/j.geomorph.2015.09.016

Rossi, P. L., Gabbianelli, G., Romagnoli, C., & Serri, G. (1990). Ricerche di geologia marina nelle aree vulcaniche del tirreno Meridionale e Canale di Sicilia. *Memorie Della Società Geologica Italiana*, *45*, 927–938.

Rossi, P. L., Tranne, C. A., Calanchi, N., & Lanti, E. (1996). Geology, stratigraphy and volcanological evolution of the island of Linosa (Sicily Channel). *Acta Vulcanologica*, *8*, 73–90.

Spatola, D., Micallef, A., Sulli, A., Basilone, L., & Basilone, G. (2018). Evidence of active fluid seepage (AFS) in the southern region of the central Mediterranean Sea. *Measurement: Journal of the International Measurement Confederation*, *128*(June), 247–253. doi:10.1016/j.measurement.2018.06.058

Tonielli, R., Di Martino, G., & Innangi, S. (2017). *Relazione allegata alla carta dei fondali dell'Isola di Linosa*. CNR-SOLAR, 14 pp. Retrieved from http://eprints.bice.rm.cnr.it/identificationcode8390BC2017, http://eprints.bice.rm.cnr.it/15948/